Structure of the liquid–vapor interfaces of Ga, In and the eutectic Ga–In alloy—an *ab initio* study

Structure of the liquid–vapor interfaces of Ga, In and the eutectic Ga–In alloy—an *ab initio* study

D J González and L E González

Departamento de Física Teórica, Atómica y Optica, Universidad de Valladolid,
47011 Valladolid, Spain

Abstract
We report the results of *ab initio* molecular dynamics simulations for the liquid–vapor interface
of the liquid metals Ga, In and the eutectic binary alloy Ga–In (16.5% In) for which
experimental data are available. The study was performed by using samples of 3000 particles in
a slab geometry with periodic boundary conditions. In those systems, the total ionic density
distributions along the normal to the interface display some layering and in the case of the
Ga–In alloy there appears a highly enriched layer of the lower surface tension component
located outermost at the interface. The results are compared with the available experimental
data.

1. Introduction

The structure of the liquid–vapor (LV) interface has attracted a considerable amount of both theoretical and experimental study [1]. Grazing incidence x-ray diffraction and x-ray reflectivity (XR) studies have been the main experimental techniques for probing the LV interface. The data obtained for several liquid metals [2, 3] (Hg, Ga, In, K) and alloys [3–5] (Na–K, Ga–In, Ga–Tl, Bi–Ga, Bi–In, Sn–Ga and Bi–Sn) have shown that the LV interface exhibits an oscillatory surface normal (longitudinal) density profile (DP) which extends several atomic diameters into the bulk liquid. Conversely, XR measurements on several non-metallic liquids [6] have evinced a DP with a smooth monotonic decay from the high-density bulk liquid to the low-density vapor.

The origin of those longitudinal ionic density oscillations has been traced back to the metallic character of the interactions in the fluid. According to Rice and co-workers [1], surface layering is caused by the coupling between the ionic and electronic densities and the abrupt decay of the electronic DP induces an effective wall-like potential against which the ions lie in an orderly way like in a hard sphere fluid close to a hard wall. However, other workers [7–9] have hinted at different scenarios such as that of many body forces, arising from delocalized electrons, which would tend to increase the ionic surface density so that its coordination resembles that of the bulk. Recently, Chacón *et al* [8, 9] proposed that surface

layering may be a generic property of fluids at low temperature, so that the only requirement for an oscillatory DP is a low melting temperature relative to the critical temperature in order to avoid crystallization.

Whatever the main cause for the surface layering, the aforementioned conjectures clearly underline the necessity for further work. In this paper we report *ab initio* molecular dynamics (MD) calculations for the LV interface in liquid Ga (l-Ga), liquid In (l-In) and the eutectic Ga–In alloy (16.5% In). Its choice was prompted by the existence of both theoretical [10–12] and experimental [2, 4] work for these systems. In the case of the liquid eutectic Ga–In alloy, the XR measurements of Regan and co-workers [4], made at temperatures $T = 298$ and 359 K, showed a strong segregation of In atoms into the outermost layer.

This study has been performed by the orbital-free *ab initio* molecular dynamics (OF-AIMD) method, where the forces acting on the nuclei are computed from the electronic structure which, in turn, is calculated within density functional theory (DFT) [13, 14]. In a metallic system, the nature of the interactions changes drastically across the LV interface and therefore it is crucial to use a formalism in which the forces on the atoms accurately reflect the electronic density distribution in their vicinity. The OF-AIMD method tackles this problem by using an explicit, albeit approximate density functional for the electronic kinetic energy. This leads to a substantial simplification from the commonly used Kohn–Sham method

Table 1. Input data along with some simulation details. L_0 is the transverse side (in Å) of the simulation box, δt is the ionic time step (in ps), E_{Cut} is the cutoff energy (in Ryd) and N_{Conf} is the total number of configurations. The σ_0^{OF}, $\sigma_{\mathrm{cw}}^{\mathrm{Exp}}$ and $\sigma_{\mathrm{cw}}^{\mathrm{OF}}$ are the different contributions (in Å) to the effective capillary roughness.

Metal	ρ_0 (Å^{-3})	T (K)	L_0	δt	E_{Cut}	N_{Conf}	σ_0^{OF}	$\sigma_{\mathrm{cw}}^{\mathrm{Exp}}$	$\sigma_{\mathrm{cw}}^{\mathrm{OF}}$
Ga	0.0512	373	33.92	0.0050	10.5	18 000	0.48	0.78	0.52
In	0.0369	450	32.53	0.0075	9.5	24 100	0.65	0.92	0.65
Ga–In	0.0550	360	31.56	0.0065	9.5	24 200	0.50	0.80	0.55

of DFT (KS-DFT) [14] which achieves greater accuracy but by imposing a much greater computational burden. The OF-AIMD method allows the simulation of large samples for long times.

2. Theory

A liquid simple metallic alloy, $A_x B_{1-x}$, can be regarded as an assembly of N_A, A-type, and N_B, B-type, bare ions with charges Z_v^A and Z_v^B respectively, enclosed in a volume Ω and interacting with $N_e = N_A Z_v^A + N_B Z_v^B$ valence electrons through electron–ion pseudopotentials $v_A(r)$ and $v_B(r)$. The total potential energy of the system can be written, within the Born–Oppenheimer approximation, as the sum of the direct ion–ion Coulombic interaction energy and the ground state energy of the electronic system, $E_g[\rho_g(\vec{r})]$. According to DFT, the ground state electronic density, $\rho_g(\vec{r})$ minimizes an energy functional which is the sum of the kinetic energy of independent electrons $T_s[\rho]$, the classical Hartree electrostatic energy $E_H[\rho]$, the exchange–correlation energy $E_{xc}[\rho]$, for which we have adopted the generalized gradient approximation and the electron–ion interaction energy $E_{ext}[\rho]$, for which we have used local ionic pseudopotentials constructed within DFT [15]. The key feature in the OF-AIMD method is the use of an explicit, although approximate functional of the density for $T_s[\rho]$, in contrast to the case for the KS-DFT method, where $T_s[\rho]$ is calculated exactly by using single-particle orbitals. We have used a functional $T_s[\rho]$ which includes the von Weizsäcker term plus further terms chosen in order to correctly reproduce some exactly known limits [15]. The local ionic pseudopotentials were constructed from first principles by fitting the displaced valence electronic density induced by an ion immersed in a metallic medium. Specifically a KS-DFT calculation was performed so as to obtain the core and valence states of the ion. Therefrom, the displaced valence electronic density is used to evaluate, within the OF-AIMD method, an effective local pseudopotential which when embedded into the metallic medium reproduces the same displaced valence electronic density. Further details concerning both the energy functional and the ionic pseudopotential are given in [15] and we recall that the present theoretical framework has provided an accurate description of several bulk static and dynamic properties as well as the LV interface in several simple metals and alloys [15–18].

3. Results

We performed OF-AIMD simulations for the LV interfaces in l-Ga, l-In and the eutectic alloy Ga–In (16.5% In) at the

thermodynamic conditions specified in table 1. For each system we have considered a slab consisting of 3000 ions in a supercell with two free surfaces normal to the z-axis. The dimensions of the slab were $L_0 \cdot L_0 \cdot \alpha L_0$ ($\alpha = 1.75$ for Ga and In and 2.0 for the alloy), with L_0 chosen so that the average ionic number density of the slab coincides with the experimental bulk value (see table 1). An additional 20 Å of vacuum were added both above and below the slab. Given the ionic positions at time t, the energy functional was minimized with respect to the (valence) electronic density $\rho(\vec{r})$, represented by a single *effective orbital* $\psi(\vec{r})$, defined as $\rho(\vec{r}) = \psi(\vec{r})^2$. The orbital is expanded in plane waves which are truncated at a cutoff energy E_{Cut}. This yields the ground state electronic density, energy, and the forces on the ions; therefrom the ionic positions and velocities were updated according to Newton equations, i.e., the simulations are performed in the NVE ensemble. For all systems equilibration runs were performed for a range between 2000 and 4000 configurations, depending on the system. Therefrom, the N_{Conf} ensuing configurations were used in the evaluation of the slab's physical properties.

The longitudinal ionic DPs were computed from a histogram of particle positions relative to the slab's center of mass. Figure 1 shows the ionic DPs obtained for l-Ga ($\rho_{\mathrm{Ga}}(z)$), l-In ($\rho_{\mathrm{In}}(z)$) and the $\mathrm{Ga}_{0.835}\mathrm{In}_{0.165}$ alloy ($\rho_{\mathrm{GaIn}}(z)$). All systems exhibit a marked stratification lasting for at least five layers, with the outer oscillation displaying the higher amplitude. All oscillations have the same wavelength, namely $\lambda = 2.5$ Å (Ga), 2.75 Å (In) and 2.55 Å ($\mathrm{Ga}_{0.835}\mathrm{In}_{0.165}$), except the outer one, which is around 16% shorter. These features qualitatively agree with the available 'experimental' and/or theoretical results. The corresponding 'experimental' DPs derived from the XR measurements [2, 4] exhibit oscillations with $\lambda \approx 2.55$ Å (Ga), 2.69 Å (In) and 2.60 Å ($\mathrm{Ga}_{0.835}\mathrm{In}_{0.165}$); moreover, the outer oscillation has also a greater amplitude than the next one. Similar characteristics were obtained in the Monte Carlo simulations of Rice and co-workers [10, 11]; specifically for l-Ga at $T = 373$ K the associated $\rho_{\mathrm{Ga}}(z)$ had a $\lambda \approx 2.5$ Å although for the alloy the corresponding $\rho_{\mathrm{GaIn}}(z)$ oscillated with a $\lambda \approx 2.9$ Å which is greater than the experimental one.

To analyze the slab's outer region we have partitioned the corresponding ionic DP into slices located between consecutive minima of the oscillations, with the outer slice stretching from the outermost minimum to the point in the decaying tail where it takes half its bulk value. By this choice, the outer slice is somewhat narrower ($\approx 16\%$) than the other slices. For both l-Ga and l-In, the outer layer has a total ionic number density greater than the bulk value ($\approx 14\%$ and $\approx 9\%$,
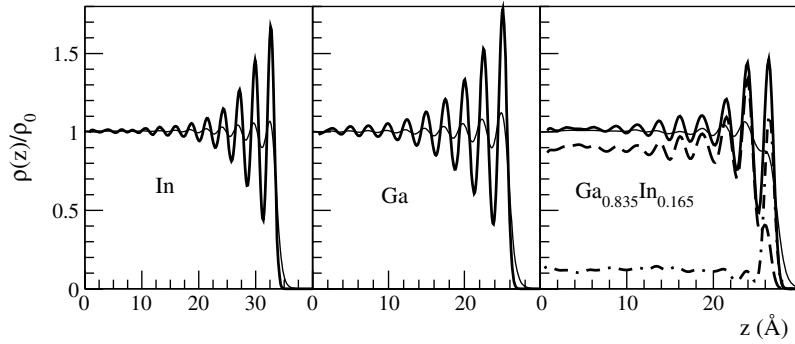
Figure 1. Electronic valence (thin line) and ionic (thick line) DPs normal to the LV interface in l-In at $T = 450$ K, l-Ga at $T = 373$ K and the Ga–In alloy at 360 K. The densities are plotted relative to the total bulk densities. In the alloy, the dashed and dash–dotted lines stand for the Ga and In partial ionic densities, respectively.

respectively) but it is ≈0% for the alloy. Conversely, at the first inner layer the change is smaller but negative (less than -1.5% in l-Ga and l-In but -3.0% in the alloy) and the following inner layers have already the bulk value, which despite its marked stratification, is attained at ≈8–10 Å from the LV interface.

The outer slice in the $\rho_{GaIn}(z)$ is strongly dominated by its partial $\rho_{In}(z)$ which is the minority component and because of its smaller surface tension is segregated to the surface and creates a high In concentration ($x_{In} \approx 0.75$) layer. We note that the combined effects of a strong surface segregation and the relatively small number of In particles used in the simulation (495 particles) give rise to a final bulk concentration, $x_{In} \approx 0.125$, which is smaller than that originally intended; in fact, the bulk value is attained at around the fourth slice, which is located at ≈10 Å from the LV interface. Similar effects were obtained in additional simulations performed for the alloys $Ga_{0.89}In_{0.11}$ and $Ga_{0.75}In_{0.25}$. The outer layers of their respective LV interfaces had $x_{In} \approx 0.58$ and 0.92 whereas, for the above mentioned reasons, their bulk concentrations were $x_{In} \approx 0.065$ and 0.21.

Some surface segregation of the component with the smaller surface tension should be expected, according to the Gibbs adsorption rule which predicts a surface concentration $x_{In} \approx 0.80$ for the eutectic $Ga_{0.835}In_{0.165}$ liquid alloy. Also, ion scattering and Auger spectroscopy measurements [19] suggest for this alloy an even larger value of around $x_{In} \approx 0.94$. These values are somewhat greater than our calculated value of 0.75; however if we use the results for the three alloys, in order to interpolate to a bulk value of $x_{In} = 0.165$, then we obtain an estimate for the associated surface concentration of $x_{In} \approx 0.83$ which, within the uncertainties posed by the interpolation, is reasonably close to the previous experimental estimates. Notice that the segregation is confined to the outer slice as the adjacent one has $x_{In} \approx 0.10$ which is depleted with respect to the bulk value; a tentative explanation for the depletion of x_{In} in the first inner slice can be traced back to the ordering tendencies exhibited by the alloy. The liquid Ga–In alloy shows some heterocoordination tendencies [19] which means that for a given atom it is energetically favorable to be surrounded by atoms of the other species; consequently given the high x_{In} values of the outer layer, there should

be expected in the adjacent layer some increase above the bulk value, in the number of Ga atoms. Conversely, an opposite trend was obtained [17] for the LV interfaces in liquid Na–K, Na–Cs and Li–Na, which are systems with varying degrees of homocoordination tendencies. For these systems it is energetically favorable for a given atom to be surrounded by atoms of same species and therefore besides a strong segregation at the outer layer, the next inner layer still exhibits a surplus, with respect to its bulk value, of the segregating species.

Further insight into the local structure is provided by the z-dependent coordination number $n(z)$. In the case of l-Ga and l-In, the $n(z)$ is defined as the average number of neighbors within a distance r_m which is taken as the position of the first minimum of the corresponding bulk pair distribution function. The results show that for most of the slab $n(z)$ remains practically constant ($n(z) \approx 12.0$ and 10.3 for l-Ga and l-In respectively) and close to the LV interface, namely around the second outer maximum, $n(z)$ begins to decrease and the previous bulk values are reduced by approximately 30% at their respective outer maximum. For the alloy, we define the partial coordination numbers $n_{ij}(z)$ ($i, j =$ Ga, In), defined as the average number of neighbors within a distance r_{ij} (identified as the position of the first minimum of the bulk partial pair distribution functions). Again, we obtain trends similar to those for the pure metals. The average bulk total number of neighbors for a Ga (In) atom stays at ≈9.7(10.7) up to around the second outer maximum in the $\rho_{GaIn}(z)$ and therefrom it decreases so that at the outer maximum takes the value ≈7.2(7.8).

Figure 1 also depicts the OF-AIMD results for the self-consistent valence electronic DP. It exhibits clear oscillations which last for a smaller range than the ionic ones and monotonically decreases at the LV interface. For all these systems we observe that the electronic oscillations are nearly in phase with the ionic ones and in [18] we already provided an explanation for this behavior.

From the calculated longitudinal total ionic DPs, we have constructed the corresponding longitudinal total electronic density DP, namely $\rho_e^T(z)$, which is depicted in figure 2 for the $Ga_{0.835}In_{0.165}$ alloy. In this calculation we have used, for each
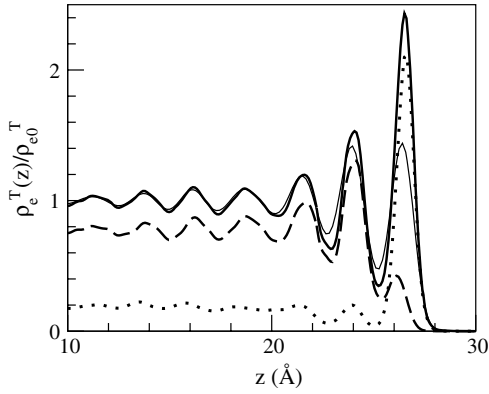
Figure 2. Total electronic density profile (core + valence) normalized to the slab's bulk value for liquid $Ga_{0.835}In_{0.165}$ (thick continuous line). The dashed and dotted lines are the Ga and In contributions to the total electronic density profiles, respectively. The thin continuous line is the total ionic density profile.

Figure 3. Fresnel normalized reflectivity for liquid Ga at 373 K (full squares, dashed ($\sigma_0^{OF} = 0.44$ Å) and dash–dotted ($\sigma_0^{OF} = 0.50$ Å) lines), In at 450 K (full diamonds and dotted line) and the $Ga_{0.835}In_{0.165}$ alloy at 360 K (full circles and continuous line). The symbols refer to the experimental data whereas the lines are the OF-AIMD based calculations. The inset shows the calculated reflectivity for the $Ga_{0.835}In_{0.165}$ alloy at 360 K (continuous line) along with its contributions from the Ga (dashed line), In (dot–dashed line) total electronic density profiles and the cross term (dotted line).

component, the respective core electronic density from the KS-DFT-type calculation performed to obtain the associated local ionic pseudopotential, whereas the valence electronic density is the total self-consistent one computed by the OF-AIMD method. Figure 2 shows that $\rho_e^T(z)$ closely follows $\rho_{GaIn}(z)$ except for the outer oscillation whose amplitude is substantially enhanced because of the increased relative contribution of In, with 46 versus 28 core electrons for Ga. Nevertheless, the oscillations in $\rho_e^T(z)$ have the same wavelength as those of $\rho_{GaIn}(z)$. Figure 2 also includes the total electronic (core + valence) DPs associated to each component of the alloy, namely $\rho_{e,Ga}^T(z)$ and $\rho_{e,In}^T(z)$. Note that for an A–B binary alloy $\rho_e^T(z) = \rho_{e,A}^T(z) + \rho_{e,B}^T(z)$.

The experimental analysis of the LV interface probes the total electronic density distribution. In the XR technique, x-rays of wavelength λ are incident upon the liquid surface at an angle α and are scattered at the same angle within the reflexion plane defined by the incident beam and the surface normal. The reflected intensity, $R(q_z)$, is
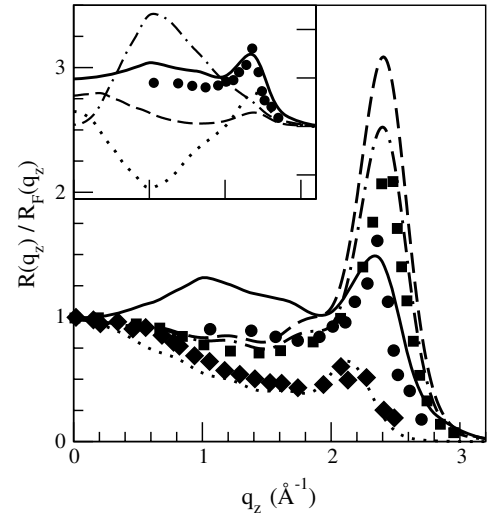
$$R(q_z)/R_F(q_z) = |\Phi_{int}(q_z)|^2 \exp(-\sigma_c^2 q_z^2) \qquad (1)$$

where $q_z = (4\pi/\lambda)\sin\alpha$, is the momentum transfer perpendicular to the interface, $R_F(q_z)$ is the Fresnel reflectivity of a perfectly sharp step function interface and $\Phi_{int}(q_z)$ is the intrinsic surface structure factor defined as

$$\Phi_{int}(q_z) = \frac{1}{\rho_{e0}^T}\int_{-\infty}^{\infty}\left(\frac{\partial\rho_{e,int}^T(z)}{\partial z}\right)\exp(iq_z z)\,dz \qquad (2)$$

where ρ_{e0}^T is the bulk total electron density and $\rho_{e,int}^T(z)$ is the *intrinsic* (i.e. in the absence of capillary wave smearing) longitudinal total (core plus valence) electronic DP. The term $\exp(-\sigma_c^2 q_z^2)$ in equation (1) purports to account for the thermally excited capillary waves, with σ_c representing an effective capillary wave roughness.

From the calculated OF-AIMD longitudinal total ionic DPs we have constructed the corresponding longitudinal total

electronic DPs, $\rho_e^T(z)$, which already include some thermal fluctuations and give a reflected intensity

$$R(q_z)/R_F(q_z) = \left|\frac{1}{\rho_{e0}^T}\int_{-\infty}^{\infty}\left(\frac{\partial\rho_e^T(z)}{\partial z}\right)\exp(iq_z z)\,dz\right|^2$$
$$\equiv \left|\frac{1}{\rho_{e0}^T}\left(\widetilde{\frac{\partial\rho_e^T(z)}{\partial z}}\right)\right|^2 \equiv |\Phi(q_z)|^2 \qquad (3)$$

where $\left(\widetilde{\frac{\partial\rho_e^T(z)}{\partial z}}\right)$ is the Fourier transform of $\left(\frac{\partial\rho_e^T(z)}{\partial z}\right)$. Comparison with equation (1), shows that the obtained OF-AIMD surface structure factor $\Phi(q_z)$ may be envisaged as the result of a convolution of the intrinsic one, $\Phi_{int}(q_z)$, with an associated Gaussian distribution describing the thermal fluctuations in the simulation.

XR measurements have been performed for l-Ga, l-In and the eutectic Ga–In alloy [2, 4], and figure 3 depicts the experimental $R(q_z)/R_F(q_z)$ curves. Therefrom, an associated ionic DP was inferred by using the 'distorted crystalline model' (DCM) in which the liquid slab is modeled by equally spaced atomic layers which become increasingly disordered as going into the bulk liquid. To account for the surface roughness, the ionic distribution of the DCM is convoluted with the Gaussian distribution $\exp(-z^2/(2\sigma_c^2))$, which by Fourier transform gives the exponential term in equation (1). The σ_c^2 has two contributions [2, 4], namely $\sigma_c^2 = \sigma_0^2 + \sigma_{cw}^2$, where σ_0 is an intrinsic surface roughness and σ_{cw} accounts for the thermally excited capillary waves [1, 2, 4]

$$\sigma_{cw}^2 = \frac{k_B T}{2\pi\gamma}\ln\left(\frac{q_{max}}{q_{min}}\right) \qquad (4)$$

where $k_B T$ is Boltzmann's constant times the absolute temperature, γ is the surface tension and q_{max} and q_{min} are determined by the ionic diameter and the instrumental resolution, respectively. A usual choice is $q_{max} = \pi/d$ with d being the ionic diameter.

On the basis of the previous ideas and using the calculated OF-AIMD density profiles, we have carried out a tentative comparison with the experimental data as evinced by the reflectivity data. First, guided by the DCM, we have quantified σ_0 by the standard deviation of the outer layer in the $\rho_e^T(z)$, leading to the values $\sigma_0^{OF} = 0.48$ (Ga), 0.65 (In) and 0.50 Å (Ga–In). Now the σ_{cw} term requires a detailed consideration because although q_{max} is the same for both the experiment and the OF-AIMD calculations, q_{min} takes different values. Specifically, whereas in the present simulations $q_{min}^{OF} = \pi/L_0$, it takes a smaller value in the experiment. This means that $\sigma_{cw}^{Exp} > \sigma_{cw}^{OF}$, namely, the experiment includes a wider range of capillary waves which must be taken into account in order to perform a meaningful comparison; consequently, the OF-AIMD reflectivity has been computed as

$$\frac{R(q_z)}{R_F(q_z)} = |\Phi(q_z)|^2 \exp\{-[(\sigma_0^{OF})^2 + \Delta\sigma_{cw}^2]q_z^2\} \qquad (5)$$

where $\Delta\sigma_{cw}^2 = (\sigma_{cw}^{Exp})^2 - (\sigma_{cw}^{OF})^2$, i.e. from the total capillary damping we subtract that part already included in the OF-AIMD simulation. Table 1 gives the concrete values used in these calculations and in figure 3 we depict the OF-AIMD reflectivity results for l-Ga, l-In and the eutectic Ga–In alloy. For all systems we obtain a fair agreement with experiment, especially for l-In. In all cases, the peak's position is correctly predicted although its height is slightly underestimated for the alloy and overestimated for l-Ga. The underestimation of the peak's height in the alloy is related to a similar underrating of the x_{In} in the outer slice of the $\rho_{GaIn}(z)$ which was explained in terms of the finite size of the simulation's slab. A greater number of particles in the slab would increase the x_{In} (and the total electronic density) in the outer slice and therefore the reflectivity's peak would also increase.

We have also found a high sensitivity of the calculated $R(q_z)/R_F(q_z)$ to the values used for the intrinsic contribution. Indeed a change of 10% in the σ_0^{OF} induces variations which are basically restricted to the peak's height and may be as large as 20%; this is evinced for l-Ga in figure 3 where we have depicted the calculated $R(q_z)/R_F(q_z)$ for $\sigma_0^{OF} = 0.44$ and 0.48 Å. Further insight into the different contributions to the alloy reflectivity can be achieved by decomposing it into different contributions. For an A–B alloy $\rho_e^T(z) = \rho_{e,A}^T(z) + \rho_{e,B}^T(z)$ and substituting into equation (3), we obtain

$$\frac{R(q_z)}{R_F(q_z)} = \left(\frac{1}{\rho_{e0}^T}\right)^2 \left[\left|\left(\frac{\widetilde{\partial\rho_{e,A}^T(z)}}{\partial z}\right)\right|^2 + \left|\left(\frac{\widetilde{\partial\rho_{e,B}^T(z)}}{\partial z}\right)\right|^2 \right.$$
$$\left. + 2\,\mathrm{Re}\left(\frac{\widetilde{\partial\rho_{e,A}^T(z)}}{\partial z}\right)^* \left(\frac{\widetilde{\partial\rho_{e,B}^T(z)}}{\partial z}\right)\right] \qquad (6)$$

where Re stands for real part and the asterisk denotes the complex conjugate. This decomposition allows us to disentangle the different contributions as originating from just

$\rho_{e,A}^T(z)$, $\rho_{e,B}^T(z)$ and a cross term. The inset in figure 3 depicts these different contributions to the alloy reflectivity. As expected from the relative concentrations in the outermost layer of the electronic DP, the main contributions arise from the In and cross terms with that from Ga playing a negligible role. This is understandable because of the very minute contribution of the $\rho_{e,Ga}^T(z)$ to the total $\rho_e^T(z)$ in the outer slice.

4. Conclusions

We have reported results of *ab initio* MD simulations for the LV interface in liquid Ga, In and the eutectic Ga–In alloy. The calculated ionic and electronic surface density profiles show marked oscillations lasting for several layers. The relative amplitudes as well as the wavelengths of the oscillations agree with the experimental data. The self-consistent valence electronic density profiles also exhibit clear oscillations which are practically in phase with the ionic ones. From the total electronic density profiles (which is the physical magnitude probed in the x-ray reflectivity measurements) we have also evaluated the associated reflected intensity, $R(q_z)$. This latter step requires us to account for the surface roughness and this is accomplished through a Debye–Waller-type factor (see equation (1)) whose main ingredient is an effective capillary wave roughness parameter σ_c. This parameter has two contributions out of which the intrinsic one σ_0 still lacks a clear meaning and we have adopted an interpretation as a measure of the width of the outer layer in the total electronic density profile, $\rho_e^T(z)$.

We end up by stressing the sensitivity of the calculated reflectivity curves to the σ_c used in equation (1). But, at the very least, the calculated reflectivity curves depicted in figure 3 show that by choosing an appropriate value for the σ_c, it is possible to provide a good description of the experimental curves over most of the q_z range. Consequently, it appears that a better understanding of the contributions to σ_c may be a basic step towards a deeper comprehension of the LV interfaces.

Acknowledgments

References

[1] Penfold J 2001 *Rep. Prog. Phys.* **64** 777
    Rice S A 2003 *Mol. Simul.* **29** 593
[2] Regan M J *et al* 1995 *Phys. Rev. Lett.* **75** 2498
[3] Tostmann H *et al* 1999 *J. Non-Cryst. Solids* **250–252** 182
[4] Regan M J *et al* 1997 *Phys. Rev. B* **55** 15874
[5] DiMasi E *et al* 2000 *J. Phys.: Condens. Matter* **12** A209
[6] Ocko B M, Wu X Z, Sirota E B, Sinha S K and
    Deutsch M 1994 *Phys. Rev. Lett.* **72** 242
[7] Iarlori S, Carnevali P, Ercolessi F and Tosatti E 1989 *Surf. Sci.* **211/212** 55
[8] Chacón E, Reinaldo-Falagan M, Velasco E and
    Tarazona P 2001 *Phys. Rev. Lett.* **87** 166101

[9] Velasco E, Tarazona P, Reinaldo-Falagan M and Chacon E 2002 *J. Chem. Phys.* **117** 10777

[10] Zhao M, Chekmarev D S, Cai Z-H and Rice S A 1997 *Phys. Rev.* E **56** 7033

[11] Zhao M, Chekmarev D S and Rice S A 1998 *J. Chem. Phys.* **109** 1959

[12] Zhao M and Rice S A 1998 *Phys. Rev.* B **57** 13501

[13] Hohenberg P and Kohn W 1964 *Phys. Rev.* **136** 864

[14] Kohn W and Sham L J 1965 *Phys. Rev.* **140** A1133

[15] González D J, González L E, López J M and Stott M J 2002 *Phys. Rev.* B **65** 184201

[16] González D J, González L E and Stott M J 2004 *Phys. Rev. Lett.* **92** 085501

[17] González D J, González L E and Stott M J 2005 *Phys. Rev. Lett.* **94** 077801

[18] González L E, González D J and Stott M J 2005 *J. Chem. Phys.* **123** 201101

[19] Dumke M F *et al* 1983 *Surf. Sci.* **124** 407